Formation of a New Archetypal Metal-Organic Framework from a Simple Monatomic Liquid

Alfredo Metere,[1, a)] Peter Oleynikov,[1] Mikhail Dzugutov,[2] and Michael O'Keeffe[3]
[1)] *Department of Materials and Environmental Chemistry, Stockholm University, S-106 91, Stockholm, Sweden*
[2)] *Department of Mathematics, Royal Institute of Technology, S-100 44 Stockholm, Sweden*
[3)] *Department of Chemistry and Biochemistry, Arizona State University, Tempe, Arizona 85287, United States*

(Dated: 19 August 2021)

We report a molecular-dynamics simulation of a single-component system of particles interacting via a spherically symmetric potential that is found to form, upon cooling from a liquid state, a low-density porous crystalline phase. Its structure analysis demonstrates that the crystal can be described by a net with a topology that belongs to the class of topologies characteristic of the metal-organic frameworks (MOFs). The observed net is new, and it is now included in the Reticular Chemistry Structure Resource database (RCSR). The observation that a net topology characteristic of MOF crystals, which are known to be formed by a coordination-driven self-assembly process, can be reproduced by a thermodynamically stable configuration of a simple single-component system of particles opens a possibility of using these models in studies of MOF nets. It also indicates that structures with MOF topology, as well as other low-density porous crystalline structures can possibly be produced in colloidal systems of spherical particles, with an appropriate tuning of interparticle interaction.

Keywords: MOF, Molecular Dynamics, Simple Monatomic Liquid, Net

I. INTRODUCTION

Thermodynamic behavior, atomic structure, properties and formation mechanisms of low-density condensed-matter phases remain a generally unexplored area. Due to the special properties of low-density porous phases, this area is in the focus of materials chemistry, materials science and statistical physics of condensed matter. Besides conceptual interest related to the peculiarities of the phase behavior of condensed-matter systems at low densities, this area presently attracts a great deal of research activity because of potentially vast scope of technological applications of porous crystalline materials. The number of newly discovered structures of such kind, which are reported every year, grows rapidly. Description, classification and design of these structurally complex materials can arguably be regarded as the last frontier of crystallography.

The current explosive growth in the number of newly created extended porous crystalline structures is a result of the development of reticular synthesis, a crystal engineering approach whereby pre-designed stable building blocks[1] are assembled into a preliminarily conceived periodic network. In particular, this development greatly advanced the synthesis of metal-organic frameworks (MOFs) that attract special interest because of the technological importance of these materials[2,3]. MOFs represent coordination networks with organic ligands containing pores that can be used e.g. for hydrogen storage, or gas separation.

The extensive research efforts aimed at the design of new MOFs raise the problem of their modelling and systematic structural characterization. The general purpose of mathematical modelling of real systems consists in reduction of the observed complexity. Reproduction of a property of an investigated system by a simplified model allows to discern its essential aspects; in this way, it makes it possible to understand the observed phenomenon by putting it in a general context which can be formalized in a respective classification. Classical crystallography is an example of such an approach: it provides a unifying description of the periodic atomic structures in terms of a general crystallographic classification, thereby reducing their compositional complexity to simplified set of archetypal geometrical model configurations.

Recently, a conceptually new approach to the description of extended periodic structures has been developed. It exploits the idea of presenting these structures in terms of topology of infinite periodic graphs (nets) which are assumed to represent the networks of bonds[1] connecting the elementary structural blocks. This is an alternative to the traditional crystallographic method of structure characterization whereby the crystalline structures are considered in terms of the geometry of configurations of points. The development of this new concept of structure description has been prompted by the advent of reticular chemistry. Using the structure description in terms of the topology of bonds, hypothetical MOFs can be redesigned from the existing structures by recombining the building blocks according to the conceived net topology[5,6].

A basic question arising in the evaluation of a hypothetical MOF model produced as a decoration of a net de-

[a)] Electronic mail: alfredo.metere@mmk.su.se

sign concerns its mechanical and thermodynamic stability. This implies that the atomic configurations designed in that way are expected to represent both potential-energy minimum, and free-energy minimum. When investigating this question, the use of a direct particle simulation of a MOF model producing a realistic atomic configuration is indispensable[7]. However, such direct simulations of MOF structures are critically constrained by the extreme complexity of the actual MOF structure. This raises a question of conceptual interest: how simple could a physical model, reproducing topology of a MOF net, be, and to what extent can the complexity of a real atomic structure described by a net be reduced? In particular, can its compositional complexity be reduced to a single-component simple system of particles?

These questions are addressed in the molecular-dynamics simulation which we describe here. It is demonstrated that a single-component system of particles interacting via a spherically symmetric potential can form a thermodynamically stable crystalline structure with a net topology that belongs to a class of nets commonly observed in MOFs. In this way, the simulation happened to produce a new archetypal MOF with a novel type of net that is now included in the RCSR database. In the following, we present a detailed description of this simulation and its results. We also discuss possible use of the general simple-system approach exploited in the present model for the topology design and analysis of other low-density porous crystalline structures, including experiments with colloidal systems.

II. MODEL AND SIMULATION

As we have explained above, the general purpose of the simulation we report here is to explore the idea of self-assembly formation of low-density porous crystalline structures in systems of identical particles using a spherically-symmetric interaction potential. For such purpose, we conceived the design of an interparticle pair potential in accordance with the following guidance concepts.

First, it is obvious that a mechanically stable energy-minimum low-density configuration of particles must necessarily possess a reduced number of neighbors in the first coordination shell, as compared with densely packed structures. In a system with a spherically-symmetric interaction, this reduction can be achieved by constraining the radial variations in the first-neighbor distance which are characteristic of the dense sphere packing. Such a constraint can be arranged by confining the first neighbors to a potential energy minimum of sufficiently reduced width.

Second, the separation between the first neighbor shell and the rest of the structure defines the configuration's density and porosity. This is controlled by the long-range repulsive branch of the pair potential. To produce this structural effect, the first minimum is supposed to be followed by a sufficiently broad maximum.

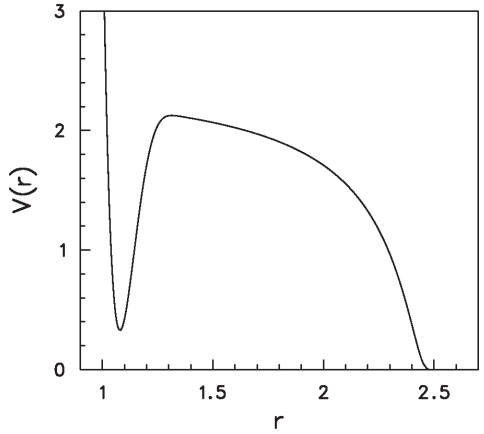

FIG. 1. Pair potential

Core-softened pair potentials possessing an additional long-range repulsion have been known to induce non-trivial phase behavior[8,9], isostructural transitions[10,11], liquid-liquid transitions, formation of clusters[12], columnar and lamellar structures[13,14]. A soft-core form of pair potential has also been found to produce formation of a glassy state[18] and a quasicrystal[19]. Isotropic soft-core potentials have also been used to produce low-coordinated structures[15–17]

These considerations were incorporated in the design of the spherically symmetric interparticle potential we exploited in this study. It is shown in in Figure 1. The functional form of the potential energy for two particles separated by the distance r is:

$$V(r) = a_1(r^{-m} - d)H(r, b_1, c_1) + a_2 H(r, b_2, c_2) \quad (1)$$

where

$$H(r, b, c) = \begin{cases} \exp\left(\frac{b}{r-c}\right) & r < c \\ 0 & r \geq c \end{cases} \quad (2)$$

The values of the parameters are presented in Table I. The first term of this functional form describes the short-range repulsion branch of the potential, and its minimum, whereas the second term is responsible for the long-range repulsion part. We remark that all the simulation results we report here are expressed in terms of the reduced units that were used in the definition of the potential. We also note that the short-range repulsion branch of the potential, and the position of its first minimum closely approximate those in the Lennard-Jones (LJ) potential[21], which makes it possible to compare directly the reduced number densities, and other thermodynamic quantities of the two systems.

We note that this pair potential represents a modification of an earlier reported one designed using the same functional form with a shorter repulsion range which was found to produce a Smectic-B crystal[20].

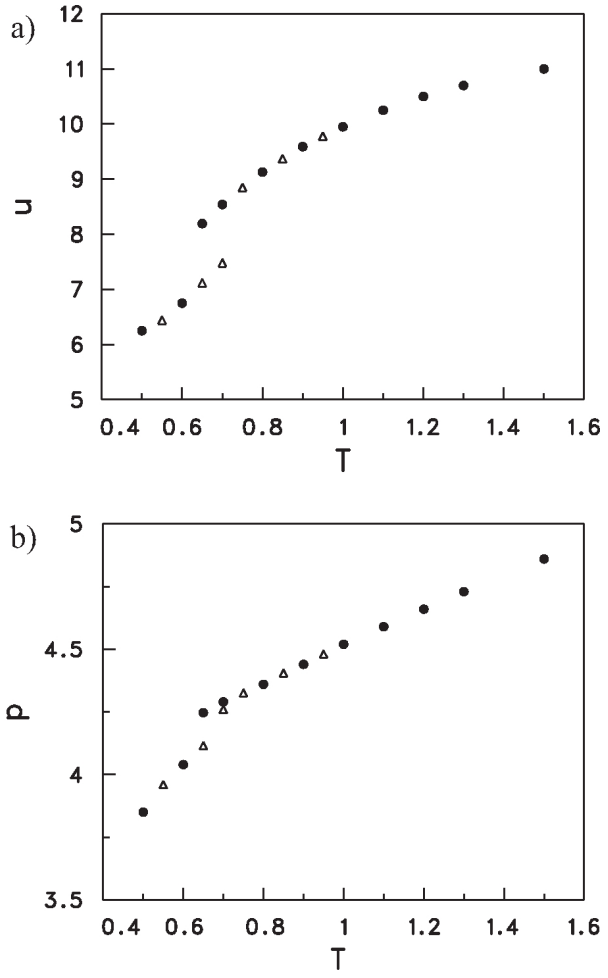

FIG. 2. Isochoric liquid-solid phase transformation. *a*) and *b*), respectively, depict energy and pressure variation as a function of temperature. Dots and open triangles correspond to cooling and heating, respectively.

m	a_1	b_1	c_1	a_2	b_2	c_2	d
12	265.85	1.5	1.45	2.5	0.19	2.5	0.8

TABLE I. Values of the parameters for the pair potential.

In this study, we employed molecular-dynamics simulation to investigate thermodynamic behavior of a system of identical particles interacting via the described pair potential at low density. The system, comprising 16384 particles, was confined to a cubic box with periodic boundary condition. The simulation was carried out at constant number density $\rho = 0.3$, in reduced units. We note that this density is very low if estimated in comparison with the LJ system phase behavior: the LJ triple-point density occurs at $\rho = 0.84$[21].

At the beginning of the simulation, the system has been equilibrated in its thermodynamically stable isotropic liquid state at sufficiently high temperature at the number density $\rho = 0.3$. The liquid was then subjected to isochorical cooling. This was performed in a stepwise manner: the system was comprehensively equilibrated at fixed temperature after each cooling step. As the liquid has been cooled below $T = 0.65$, a discontinuous change in the thermodynamic parameters was detected, which can be seen in Fig. 2. The thermodynamic singularity was found to be accompanied by a sharp drop in the rate of self-diffusion. These observations represent an apparent signature of a first-order phase transition to a solid phase. The conclusion was further confirmed by a significant hysteresis that was produced when heating the low-temperature phase. A non-trivial character of the low-temperature phase was indicated by an anomalously long time required for its equilibration which amounted to several billions of time-steps.

III. RESULTS

A. Structure

We now turn to characterization of the simulated structure, and try to understand its relationship with the pair potential. In order to facilitate the structure characterization, we analyzed an energy-minimum configuration. For that purpose, the steepest-descent minimization procedure was applied to a system's instantaneous configuration thereby reducing the system to its nearest potential-energy minimum. In this way, the configuration was rid of any thermally induced perturbations.

The structure was first inspected in terms of one-dimensional correlation functions, the radial distribution function, $g(r)$, and its reciprocal-space counterpart, the spherically-averaged structure factor $S(Q)$ which are related as:

$$S(Q) = 1 + 4\pi\rho \int_0^\infty [g(r) - 1] \frac{\sin(Qr)}{Qr} r^2 dr \qquad (3)$$

These correlation functions are presented in Fig. 3. An apparent anomaly featured by the calculated $g(r)$ is a big gap between the first and the second meaningful maximum; the latter occurs at the distance of about $r = 2.5$. The big separation distance to the second shell of neighbors, anomalous for a dense sphere packing, can be associated with the characteristic void size in a porous structure. Accordingly, $S(Q)$ features a singularly sharp peak at the Q-value corresponding to the indicated distance, which can apparently be regarded as a characteristic length-scale of this porous configuration.

Further insight into the origin of these structural peculiarities can be obtained from the analysis of the Fourier-space distribution of the structure factor $S(\mathbf{Q})$. The latter is calculated as:

$$S(\mathbf{Q}) = \frac{1}{N} \langle \rho(\mathbf{Q}) \rho(-\mathbf{Q}) \rangle \qquad (4)$$

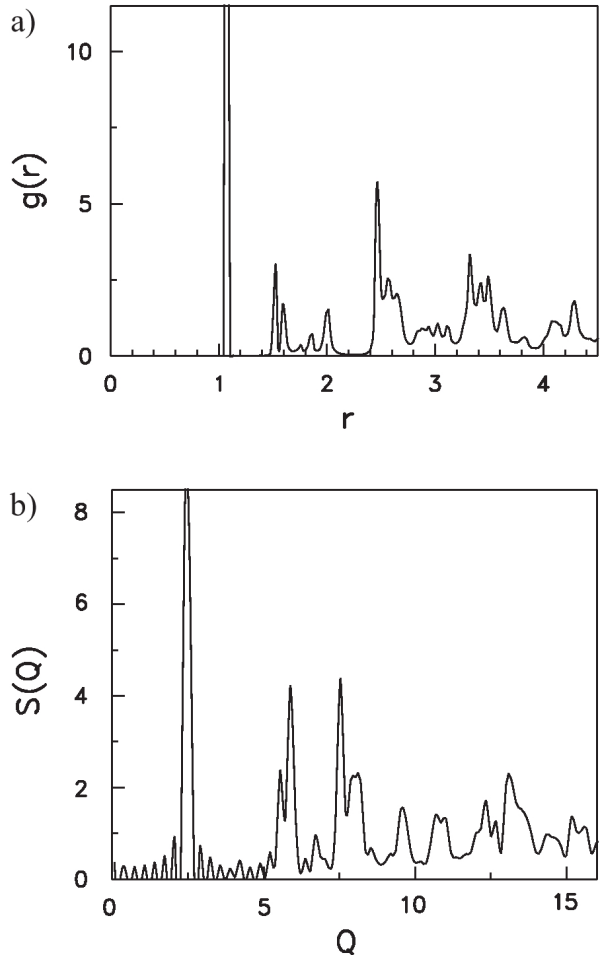

FIG. 3. *a*) Radial distribution function. *b*) Spherically averaged structure factor.

where $\rho(\mathbf{Q})$ is a Fourier-component of the system's number density:

$$\rho(\mathbf{Q}) = \sum_{j=1}^{N} \exp(i\mathbf{Q}\mathbf{r}_j) \tag{5}$$

$\mathbf{r}_i$ being the positions of the system's particles, and N is the number of particles in the system. Notice that $S(\mathbf{Q})$ represents the signal intensity as measured in diffraction experiments.

As a first step, we calculated the diffraction intensity on the Q-space sphere of diameter corresponding to the position of the sharp pre-peak of the spherically averaged $S(Q)$, see Fig. 3. This result is shown in Fig. 4(a). It demonstrates that the pre-peak decomposes into a set of well-defined diffraction maxima which form a regular four-fold pattern. This made it possible to determine the global symmetry of the configuration, which is found to be characterized by a single four-fold axis. The axis orientation having been determined, we calculated $S(\mathbf{Q})$ within two characteristic Q-space planes: $Q_z = 0$ and $Q_y = 0$, Q_z being the axis coordinate, and Q_y coordinate corresponding to a translational symmetry vector

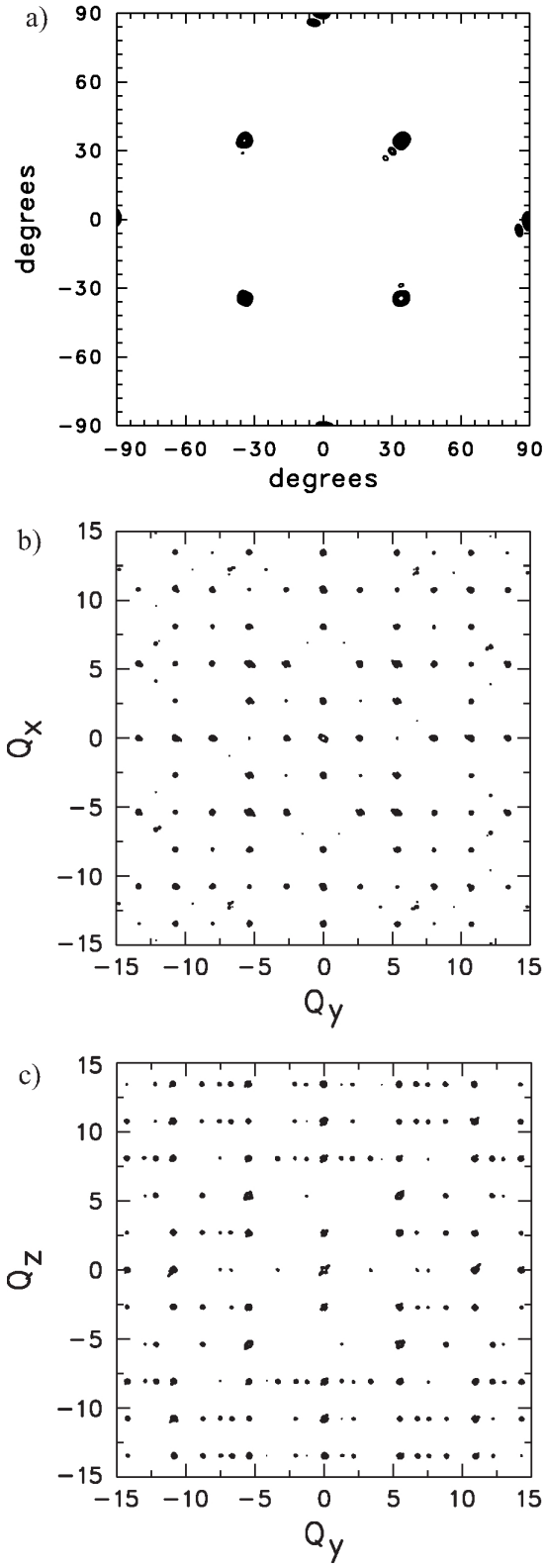

FIG. 4. The isointensity plots of the structure factor $S(\mathbf{Q})$. *a*) Diffraction intensity in the reciprocal-space sphere of the radius $Q = 2.5$ which corresponds to the position of the sharp pre-peak of $S(Q)$ in Fig. 2, as viewed from the axial direction. *b*) In the reciprocal-space plane orthogonal to the axis, $Q_z = 0$. *c*) In the axially oriented plane, $Q_y = 0$. Q_z denotes the axial dimension, and Q_y corresponds to a translational symmetry vector, orthogonal to the axis.

orthogonal to the axis. These two diffraction planes are also shown in Fig. 4(b, c).

The pattern of diffraction maxima presented in Fig. 4 is visibly dominated by the characteristic spacing $\Delta Q = 2.5$ that has been detected as the position of the first sharp peak of $S(Q)$ in Fig. 3. This feature we attributed to the presence of voids with characteristic spacing of about 2.5 atomic diameters. It can thus be concluded that these voids represent the dominating element of the investigated structure, forming a periodic pattern with single four-fold axis.

B. Description of the real-space configuration of our simulated structure

In this section we present a real-space description of the simulated phase structure. We discern its unit cell and demonstrate the structure's porosity which was conjectured in the previous section from the diffraction pattern.

The particle configuration, representing the simulated crystal, is confined to a cubic simulation box with periodic boundary conditions. We note that the crystal is misaligned with respect to the coordinate axes of the confining box.

As the first step of the real-space structure characterization we describe the correlations of the particle positions in terms of the radial distribution function (RDF). The short-range part of this function is presented in Fig. 5. The distribution reveals a set of peaks that represent the characteristic distances between the nearest neighbors. Two of these peaks, highlighted in Fig. 5 by colors, represent two ranges of interparticle distances which are defined as the basic bonds forming the structure. The simulated crystal is then described as a network of these bonds.

Next, we consider thus defined network of bonds to discern the unit cell the periodic repetition of which in three dimensions forms the simulated crystal structure. The unit cell configuration is shown in Fig. 6. Its bonds are colored in the same manner as that used to highlight the respective peaks of the radial distribution function shown in Fig. 5.

The unit cell parameters and the positions of the asymmetric unit vertices, scaled by the size of the unit cell are reported in Table II. These were estimated in terms of the interparticle distances corresponding to the maxima of the highlighted peaks in Fig. 5. The unit cell is tetragonal and has $P4_2/mnm$ symmetry, which explains why there are only two vertices in the asymmetric unit.

Connecting particles with bonds of $r_1 \approx 1.08$ length will generate a regular octahedron in the middle of the unit cell. Such bonds correspond to the first peak position in the radial distribution function which is related with the 3D periodic pattern. Bonds of the length $r_2 \approx 1.63$ will connect the central octahedron with its symmetry-related replicas located at the corners of the

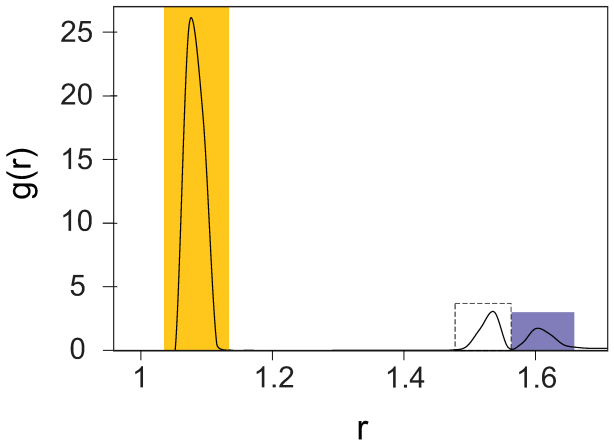

FIG. 5. Portion of the radial distribution function of the simulated crystal configuration. Highlighted are the distance ranges corresponding to the peaks which are used as bonds defining the unit cell Fig. 6. Yellow and purple, respectively, depict the peaks positioned at $r_1 \approx 1.08$ and $r_2 \approx 1.63$.

Space group	$a = b$	c	$\alpha = \beta = \gamma$
$P4_2/mnm$	3.600	3.200	90°

Vertex	x/a	y/b	z/c
V_1	0.39342	0.39342	0.33077
V_2	0.14994	0.14994	0

TABLE II. Reconstructed unit cell parameters and list of the vertices in the asymmetric unit, scaled by the unit-cell size.

unit cell.

The four basal particles of each octahedron are 5-coordinated, while the two apical particles are 6-coordinated. A graphical representation of the unit cell with the particles connected according to the described bonding scheme is shown in Fig. 6.

The peak region presented in the radial distribution function (see Fig. 5) as the dashed region corresponds to the interparticle distances distribution representing the solid (volume) diagonals of the octahedra. However, we did not take this peak region into the account when constructing the bond network because the resulting bonds would intersect with each other in the centers of the octahedra.

A fragment of the simulated crystal configuration presented as a network of bonds is shown in Fig. 7. By considering the sequences of adjacent unit cells it is possible to notice how their self-repetition along the unit cell axes generates a mono-dimensional channel system which develops along the Z-axis. The pore diameter is estimated as $\phi \approx 2.5$, which is comparable with the size of the unit cell. We also remark that the pore diameter is consistent, as anticipated, with the ultimate distance of the second (longer-range) repulsion part of the pair potential.

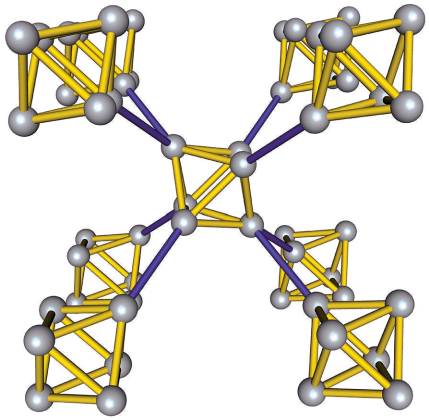

FIG. 6. The unit cell of the simulated crystal configuration. The yellow and purple bonds correspond to the distance ranges higlighted by similar colors in Fig. 5

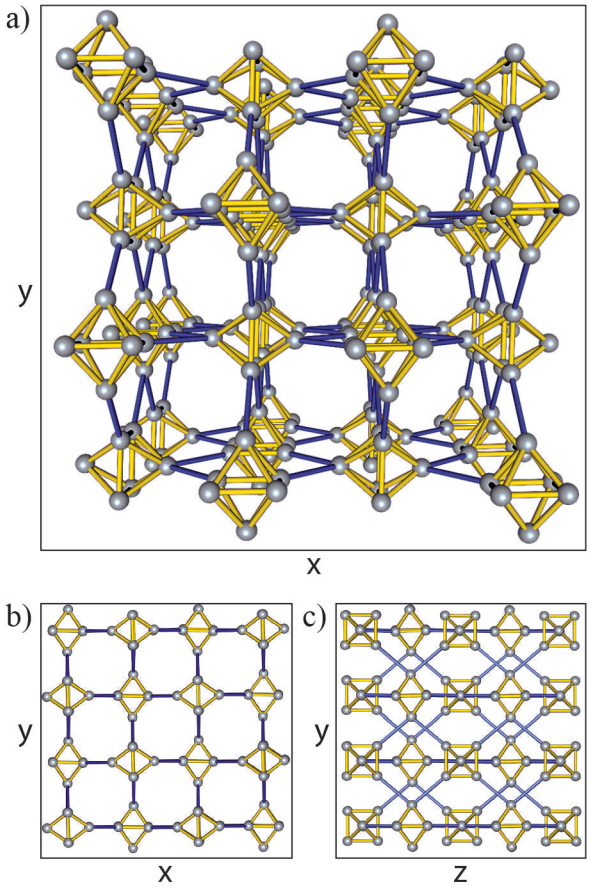

FIG. 7. A fragment of the simulate crystal configuration produced using the same bonding method as used for the unit cell plot in Fig. 6, using the same respective bond colors. *a*) Perspective projection demonstrating how the octahedra are interconnected to form the pores. *b*) and *c*): orthogonal projections.

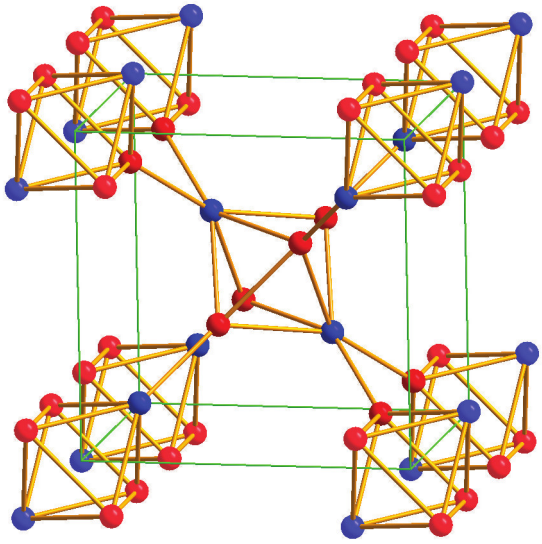

FIG. 8. The unit-cell configuration for the 'alm' net included in RCSR classification[22], its parameters presented in Table III (see explanations in the text)

It is not directly possible to assess the class of real materials which our simulated crystal structure belongs to. This is because the definitions of micro-, meso- and macro-porosity are related to the size of the pore diameter expressed in explicit units rather than reduced units. Proceeding by exclusion we can assert that our structure does not belong to any known zeolitic, Covalent Organic Frameworks (COFs) and Zeolitic Imidazolate Frameworks (ZIFs) types, because of the coordination numbers of its particles. The periodically ordered pore walls indicate that our structure is not to be classified as crystalline mesoporous silica either. Excluded this way the other candidates, we conclude that our structure is of a new archetypal MOF.

C. The net classification

We now turn to the topological classification of the bond network of our simulated particle configuration. Our structure exhibits a novel topology (net) that has been included in the Reticular Chemistry Structure Resource (RCSR) database[22] where it is named '**alm**'. That crystal net produced using the method of bonding that we described above is shown in Fig. 8. The connectivity of the nodes in this unit cell is exactly the same as was observed in the the unit cell of the simulated structure shown in Fig. 6. The only difference between the two unit cells configurations is that in the one shown in Fig. 8 all the bond length values have been we normalized to 1. The '**alm**'-net unit cell parameters and the asymmetric unit vertices are presented in Table III.

Space group	$a = b$	c	$\alpha = \beta = \gamma$
$P4_2/mnm$	2.7818	2.3002	90°

Vertex	x/a	y/b	z/c
V_1	0.3729	0.3729	0.2826
V_2	0.1797	0.1797	0

TABLE III. Unit cell parameters and vertices of the 'alm' net included in the RCSR classification[22].

IV. CONCLUSIONS

The simulation results we report here demonstrate that a thermodynamically stable, low-density, microporous, crystalline phase, exhibiting a kind of topology characteristic of the MOF nets, can be formed by a single-component system of particles with a spherically-symmetric interaction.

A more general conclusion of this study is that the form of pair potential we explored here can be further exploited to simulate other novel extended low-density porous crystalline structures, including those with MOF topologies. This approach can possibly be regarded as complementary to the mathematical efforts, in exploring the topological variety of possible reticular chemistry structures.

Another perspective application of this simulation is that it can be used as a guidance for creating similar structures in colloidal systems of spherical particles with appropriate tuning interparticle force field. It has to be mentioned that the main features of the pair potential we exploited in this simulation are consistent with the classical theory for colloidal interactions by Deryagin, Landau, Verwey and Overbeek (DLVO)[23–26], amended with hard-core repulsion or steric repulsion close to the contact.

V. ACKNOWLEDGMENTS

The authors thank Sten Sarman for illuminating discussions. The simulations were performed using the resources provided by the Swedish National Infrastructure for Computing (SNIC) at PDC Centre for High Performance Computing (PDC-HPC).

[1] D.J. Tranchemontagne, J.L. Mendoza-Cortes, M. O'Keeffe, and O. M. Yaghi, Chem. Soc. Rev. **38-5**, 1257 (2009)
[2] B. Wang, A. P. Ct, H. Furukawa, M. O'Keeffe, and O. M. Yaghi, Nature **453**, 207 (2008)
[3] R. Banerjee, A. Phan, B. Wang, C. Knobler, H. Furukawa. M. O'Keeffe, and O. M. Yaghi, Science **319**, 939 (2008)
[4] M. O'Keeffe, Chem. Soc. Rev. **38**, 1215 (2009)
[5] M. O'Keeffe, and O. M. Yaghi, Chemical Reviews **112**, 675 (2012)
[6] C. E. Wilmer, M. Leaf, C. Y. Lee, O. K. Farha, B. G. Hauser, J. T. Hupp, and R. Q. Snurr, Nature Chemistry **4**, 83 (2012)
[7] F.A. Cabrales-Navarroa, J.L. Gmez-Ballesterosa, and P.B. Balbuena, Journal of Membrane Science **428**, 241 (2013)
[8] Yu. D. Fomin, E. N. Tsiok, and V. N. Ryzhov, J. Chem. Phys. **134**, 044523 (2011)
[9] Yu. D. Fomin, N. V. Gribova, V. N. Ryzhov, S. M. Stishov, and D. Frenkel, J. Chem. Phys. **129**, 064512 (2008)
[10] P.C. Hemmer and G. Stell, Phys. Rev. Lett. **24**, 1284 (1970)
[11] G. Stell and P. C. Hemmer, J. Chem. Phys. **56**, 4274 (1972)
[12] J. Dobnikar, J. Fornleitner, and G Kahl, J. Phys. Cond. Matter **20**, 494220 (2008)
[13] G.J. Pauschenwein, and G. Kahl, J. Chem. Phys. **129**, 174107 (2008)
[14] G.J. Pauschenwein, and G. Kahl, Soft Matter 4, 1396 (2008)
[15] S. Torquato, Soft Matter,**5**, 1157 (2009)
[16] S. Prestipino, F. Saijab and G. Malescio, Soft Matter, **5**, 2795 (2009)
[17] G. Zhang, F. H. Stillinger, and S. Torquato, Phys. Rev. E **88**, 042309 (2013)
[18] M. Dzugutov, Phys. Rev. A **46**, R2984 (1992)
[19] M. Dzugutov, Phys. Rev. Lett. **70**, 2924 (1993)
[20] A. Metere, T. Oppelstrup, S. Sarman, A. Laaksonen, and M.Dzugutov, Phys. Rev. E, **88**, 062502 (2013)
[21] J. P. Hansen, and I. R. McDonald, Theory of simple liquids (2013)
[22] http://rcsr.anu.edu.au/nets/alm
[23] B. Derjaguin and L. Landau, Acta Physico Chemica URSS **14**, 633 (1941)
[24] E. J. Verwey, and J. Th. G. Overbeek, Theory of the stability of lyophobic colloids (1948)
[25] J. N. Israelachvili, Intermolecular and Surface Forces (2011)
[26] G. Malescio, Nature Materials **2**, 501 (2003)